Peer-reviewed version available at *Materials* **2020**, *13*, 2749; doi:10.3390/ma13122749

Article

Introduction of a Methodology to Enhance the Stabilization Process of PAN Fibers by Modeling and Advanced Characterization

George Konstantopoulos[1], Spyridon Soulis[1], Dimitrios A. Dragatogiannis[1], Costas A. Charitidis[1,*]

[1] Research Unit of Advanced, Composite, Nano Materials & Nanotechnology, School of Chemical Engineering, National Technical University of Athens, Department III, 9 Heroon Polytechniou str., Zografou Campus, 157 73 Athens, Greece

* Correspondence: charitidis@chemeng.ntua.gr

Abstract: A methodology is proposed for designing the stabilization process of polyacrylonitrile (PAN) fibers. In its core, this methodology is based on a model that describes the characteristic fiber length change during the treatment, through the de-convolution of the three main contributors (i.e. entropic shrinkage, creep, and chemical shrinkage). The model has the additional advantage of offering further insight into the physical and chemical phenomena taking place during the treatment. Validation of PAN-model prediction performance for different processing parameters was achieved as demonstrated by FTIR and DSC. Tensile testing revealed the effect of processing parameters on fiber quality, while model prediction demonstrated that ladder polymer formation is accelerated at temperatures over 200ºC. Additionally, according the DSC and FTIR measurements predictions from the application of the model during stabilization seem to be more precise at high-temperature stabilization stages. It was shown that mechanical properties could be enhanced preferably by including a treatment step below 200ºC, before the initiation of cyclization reactions. Further confirmation was provided via Raman spectroscopy, which demonstrated that graphitic like planes are formed upon stabilization above 200ºC, and thus multistage stabilization is required to optimize synthesis of carbon fibers. Optical Microscopy proved that isothermal stabilization treatment did not severy alter the cross section geometry of PAN fiber monofilaments.

Keywords: polyacrylonitrile; stabilization; cyclization; kinetics; carbon fiber

1. Introduction

The increasing demand in carbon fiber reinforced plastics (CFRPs) in many sectors such as aeronautics/space engineering, automotive, construction, and sport equipment highlights the relative importance of further improving and optimizing the production process and surface chemistry of carbon fibers (CF) in order to fabricate cost- and energy-efficient composites [1-3]. This can be better achieved by modifications of the stabilization process [4-10], since carbonization is a straightforward process that cannot be essentially altered and that investigation on novel CF precursors is time a consuming procedure. PAN-based CFs are more efficiently manufactured (due to their high carbon yield) and demonstrate a structure with less defects and voids, affording CF with high tensile strength in comparison to CFs derived from pitch, Rayon, or renewable precursors [1,10-15]. Given that PAN-based CFs represent about 80-90 % of the world production, there is a strong incentive for improving the process design, so that it might be further optimized [9,14,16].

Stabilization is considered as the most crucial step; obtaining a proper structure is critical for achieving high performance CFs. This oxidation step, leads to an infusible and inflammable ladder polymer structure, suitable for carbonization [11,14,17-19]. Regarding the thermal treatment, processability of PAN fibers is enhanced at temperatures exceeding glass transition temperature (T_g), commonly above 170ºC [20]. In this temperature region the PAN precursor is partially plasticized and this is the point where an improvement in fiber orientation could be achieved, while tension

assists the process and leads to enhanced molecular alignment in fibers [21-23]. Molecular structure is affected by several reaction pathways that transform the polymer backbone of fused heteroaromatic structures; furthermore, the presence of heteroatoms such as residual hydrogen, nitrogen and oxygen can lead to crosslinking, and thus to higher carbon yields and an improved structure upon carbonization [6,11,24-28].

During stabilization process, physical and chemical transformations occur that can be observed by the change in fiber length. The latter is dominated by three phenomena, namely: entropic shrinkage, creep and chemical shrinkage [21,29,30]. Recently, it was proposed to utilize the length change for the in depth investigation of the stabilization process; this approach is based on the deconvolution of the corresponding phenomena that take place during the process. Entropic shrinkage (ES) or recovery is a physical transformation that occurs at early stabilization stages upon initiation of stabilization reactions. It is attributed to relaxation of highly orientated PAN macromolecules, due to the spinning and post-spinning treatment and the reduction of crystalline regions during thermal treatment. It was found that maximum Entropic Shrinkage (ES_{max}, i.e. the shrinkage of the PAN fibers in the primal stage of thermal treatment in the limiting case where no stress is applied), is a physical constant that depends on the structure of the PAN homo/co-polymer fiber [1]. It is explained on the basis of the helical form of PAN molecule with intermolecular repulsive forces between the adjacent nitrile group dipoles [23]. Stretching of the fibers during their manufacture develops strains in the molecules which relax during heat treatment, and consequently the fiber shrinks [1,21,31,32]. In contrast to entropic shrinkage, creep is a heat activated phenomenon which is dependent on temperature and applied stress. These parameters can be adjusted in order to prevent shrinkage, retain post-spinning treatment orientation, and further orientate PAN molecules [21,22,27,31,33]. However, application of a very high-tension during stabilization may disturb the preferred orientation required for the cyclization reaction by causing bonds rupture, and thus lead to reduction of mechanical properties [1,13,23,34]. Chemical shrinkage occurs as a result of exothermic chemical reactions during the stabilization process, which lead to the formation of cyclized ladder polymer, and it was shown that it could be used as a measure of the nitrile cyclization reaction progress [1,23,32]. The rate and magnitude of this shrinkage depends on factors such as the atmosphere, the stabilization temperature, the applied stress, the stretch given to the precursor fiber during spinning process, as well as the heating rate [1,13,23,35].

Generally, the main chemical reactions that occur during stabilization are dehydrogenation, cyclization and oxidation; their initiation depends on the treatment temperature, which also determines the relative effect and the relative rate of each reaction at the specific treatment stage [7,11,13,14,23,28,31,36]. Dehydrogenation reactions are considered to precede cyclization, while the oxidation takes place in the whole temperature region of stabilization. These reactions are responsible for the gradual change in colour of the precursor fiber, starting from white to yellow, to brown, and ultimately to black [23,37]. The colour change is assumed to be result of polyene structures produced during heat treatment of PAN, while it is also claimed that black colour appears due to formation of a condensed ring structure containing carbon-nitrogen double bonds (Figure 1), known as ladder structure. Preheating of PAN fibers in air initiates dehydrogenation reaction, resulting in formation of double bonds in the chain backbone which imparts greater stability to the chain [7,28].

Peer-reviewed version available at Materials 2020, 13, 2749; doi:10.3390/ma13122749

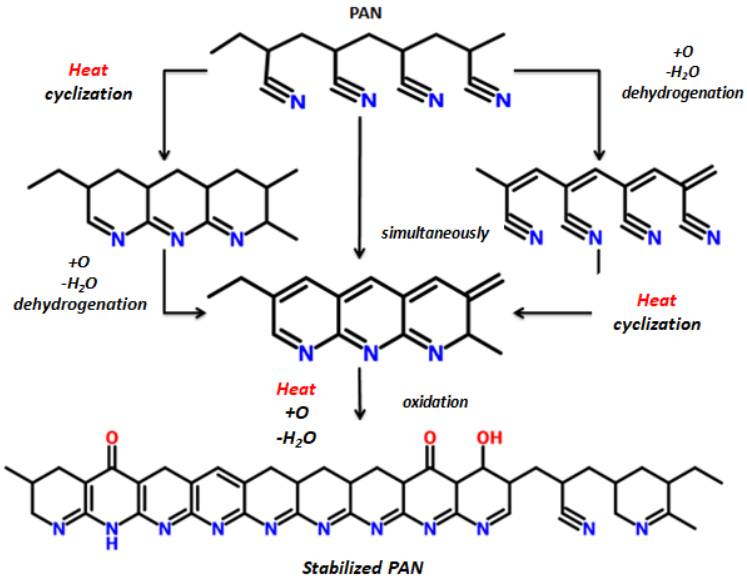

Figure 1. Sequence of reactions during thermooxidative stabilization of PAN precursor.

Cyclization is considered the main stabilization reaction, with its importance increasing by raising temperature in the region from 180 to 250°C. The end products are various imine structures among PAN macromolecules though oligomerization of nitrile groups, via linkage between nitrogen and the carbon atom of the succeeding nitrile group of the chain [7,11]. Cyclization is initiated at several activation points of PAN molecule during heat treatment, and evolves until its growth is terminated by reaching another conjugated or cyclized unit [23]. Several reaction mechanisms have been proposed in the literature, based on either self initiation (mainly in the case of copolymers with oxygen-containing comomnomers that act as initiation points) or on external initiation (from the attack of the oxygen on the polymer backbone) [23,38]. Initiation occurs via a radical mechanism in the homopolymer and through an ionic mechanism in copolymers; however, the reaction mechanism (or even the sequence of the reactions) does not really affect the structure of stabilized PAN fibers [6,13,23]. However, it is widely accepted that chemical shrinkage, is induced exclusively by the nitrile cyclization reactions [19,39,40].

Cyclization is followed by higher temperature oxidation, in order to derive the final pyridine structure. Generally, oxidation has a twofold effect on the stabilization process: on the one hand, oxygen initiates the formation of active centers for cyclization above 240°C as oxygen diffusion is the dominating pathway for the transformation of the PAN fibers [13,23]. It has also been stated that at elevated temperatures, oxidation reaction occur at a higher rate than cyclization, even though between 180°C and 240°C cyclization is the dominating reaction [1,7]. However, it has been reported that further aromatization and intermolecular crosslinking reactions occur in the fiber while performing oxidative stabilization at 300-400°C (Figure 2). This leads to formation of highly ordered and compact structural units in the stabilized fiber (Figure 3) [23,24]. Molecular chains in the fiber undergo realignment, reorientation, and reinforcement along the fiber axis, to form pockets of small-sized basic structural units that maintain a crystalline distance of 6.8 Å [23]. As the stabilization temperature increases, the repeat units grow in number and size.

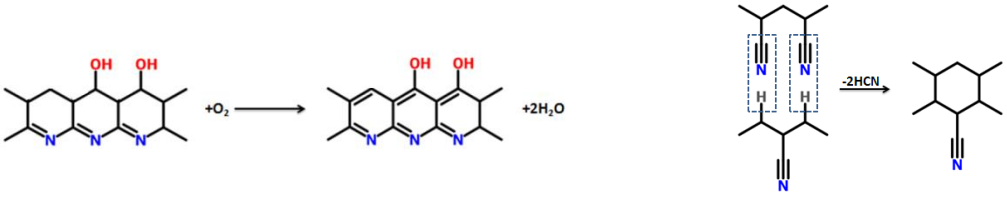

(a) (b)

Figure 2. Reactions in presence of oxygen at 300-400°C of (a) Aromatization, and (b) Intermolecular cross-linking.

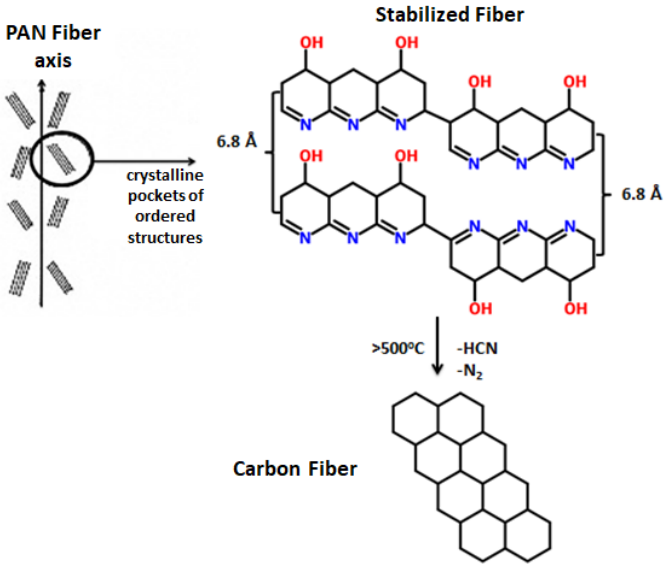

Figure 3. Carbonization mechanism of PAN fibers.

In most case studies the object of stabilization investigation is the description of reaction mechanisms and the effect on structural changes; using microscopy, spectroscopy, and thermal analysis kinetic studies on cyclization and oxidation are performed, and progress of the reactions (e.g. cyclization) is estimated [19,29,30,39,41]. While this approach seems time consuming, industrial scale stabilization can be better optimized through a combination of time-consuming experimentation, together with the application of empirical laws that relate temperature, tension, and time with the mechanical properties of the resulting CFs [28].

The aim of this work is to develop a comprehensive model that will describe the length change during the oxidative thermal stabilization of PAN fibers in the whole space of treatment variables (temperature, time and applied stress) and correlate it with the structural changes. Such a model could use the length change during the process as an effective control parameter. The fundamental idea for the model is to isolate the effect of each phenomenon on the change in fiber length, as well as to establish the relation between length variation and stabilization parameters for each one of these phenomena. Since the correlation between cyclization and chemical shrinkage has been well established, the latter can be used as a measure to quantify the estimation of the stabilization progress, given that cyclization is considered as the most crucial reaction during the formation of the ladder polymer. By using the extracted model, it is expected that the number of the necessary experiments for optimizing the process will be minimized. Fourier Transform Infrared Spectroscopy (FTIR) and Differential Scanning Calorimetry (DSC) were used to quantify cyclization yield and compare to the model. Further characterization was also performed to identify structural transformations during stabilization, such as optical microscopy in order to measure the deviation from circularity of fiber cross section.

2. Materials and Methods

2.1 Materials

Polyacrylonitrile (PAN) copolymer fiber yarns were obtained by Yataida Ltd (YTD PAN fibers), China, consisting of 1000 filaments. The YTD PAN fibers and were not subjected to any treatment prior to stabilization.

2.2 Isothermal Stabilization Process

Stabilized fibers were synthesized by thermal treatment in a stabilization furnace apparatus with internal air circulation, temperature control, and load adjustment capability. In order to be able to measure the length variation during the treatment, the fibers were inserted in the oven using a proper frame. To enhance reproducibility, the samples that were prepared for stabilization had the same initial fiber length and were hanged on the frame on pre-specified positions (i.e. their position inside the stabilization oven is well defined). Specimens were heated isothermally in the temperature range between 160-270^{o}C, with the applied tension ranging between 0.07 and 22MPa for different process time, which could be extended depending on the needs of modeling stabilization kinetics for the copolymer fiber.

2.3 Characterization of Stabilized YTD PAN fibers

Fourier Transform Infrared Reflectance (FTIR) analysis was performed using KBr pellet technique on a Cary 630 spectrometer (Agilent) with operating wavelength in the range of 4000-400 cm^{-1} and resolution of 4 cm^{-1}. Samples were dried overnight at 60^{o}C, and stabilized PAN fibers were grinded with KBr powder at 2% wt mixing ratio. Then, the powder was pressed into pellets and measured using the proper FTIR transmission module. Raman spectroscopy was performed using *InviaH-Renishaw* argon laser with wavelength 514.5 nm (Green) and laser beam size of ~ 2 μm of diameter. ×50 magnification microscope and 10-second exposure with 5 accumulations for each scan were used. Extended scans from 100 to 3500 cm^{-1} were performed to obtain both the first- and second-order Raman bands of the carbon materials. Laser power was set at 0.3 mW, 5% of the maximum available power of 6 mW. The correction with respect to the quantum efficiency of detector and the baseline correction have been applied using MATLAB software. In order to make the comparisons, all the spectra normalized to the D peak at 1372 cm^{-1}.

Thermal analysis was carried out using a NETZSCH thermal analysis system. Simultaneous TG-DTA/DSC was performed using the STA 449 F5 Jupiter Apparatus, which can execute both Thermogravimetric Analysis (TGA) and DSC. The system consists of a Silicon Carbide Furnace with temperature range from 25^{o}C to 1550^{o}C, SiC heating element and Al_2O_3 protective tube for gas flow with stop valve. TGA experiments were conducted using N_2 or synthetic air flow (mix of 80% N_2 and 20% O_2) of 50 mL/min, and a heating rate of 5 ^{o}C/min. PAN samples were oxidatively stabilized in a thermal furnace apparatus under 300g of applied load for 4h, in the temperature range of 160^{o}C to 270^{o}C (isothermally), prior to characterization.

In order to investigate any deviation in cross-section circularity of PAN fibers induced by stabilization, OM was performed using a Mighty Scope 500× Digital Microscope, while Image analysis software was used named ImageJ. For OM investigation, four monofilamens were selected from each strand with random sampling. The aim of this investigation was to study the variation in PAN fiber cross-section after the stabilization treatment, considering that fiber circularity may be affected by extreme temperature and stress conditions. Prior to their measurement, the samples were encapsulated using a commercial polymer in powder form and a suitable organic solvent was used at a 1:1 ratio to produce a liquefied resin. The resin was hardened for 24h followed by grinding progressively with decreasing granulometry reaching a final grain size of 10 μm

3. Results and Discussion

3.1 Modeling of Entropic Shrinkage (ES)

The non-linear thermoplastic behavior of the PAN fibers can be clearly seen by plotting isothermal and isochronous change of length versus the applied stress (**Figure 4**a). However, the lower part of the curves (i.e. for applied stress up to 5 MPa) shows a linear dependence between shrinkage and tension, indicating that PAN can be considered as a linear viscoelastic material at this region [42]. The intercept of the straight line represents the maximum value of shrinkage achieved under "free shrinkage" conditions (i.e. with no applied stress, σ=0) for that temperature - time

combination [1]. This value is termed entropic shrinkage (ES), since it can be directly related to the irreversible entropic recovery of the fibers (since the macromolecules of PAN revert from a highly oriented structure to the random coil configuration) [30,43]. At each temperature, it was proven that ES gradually increases until reaching a maximum value after some time.

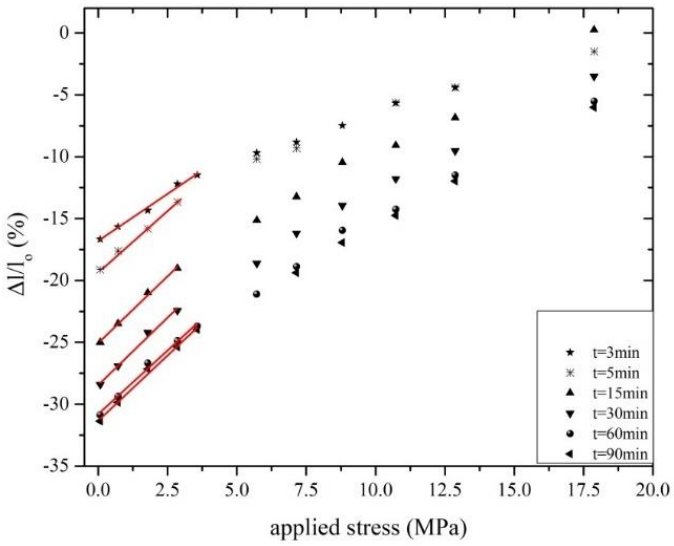

(a)

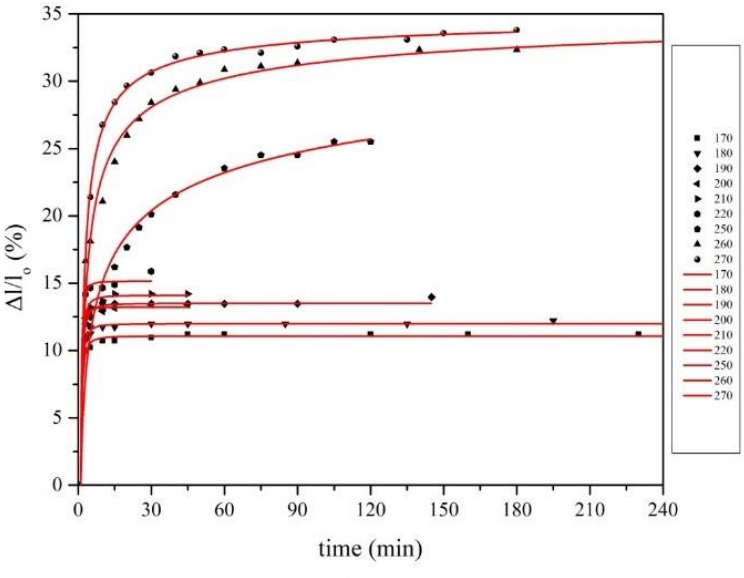

(b)

Figure 4. (a) Isochronous change of length during isothermal stabilization, (b) Entropic shrinkage versus treatment time for YTD PAN fiber at different temperature.

In Figure 4b, typical ES-time curves are presented. It was possible to fit the ES-treatment time points using non-linear regression, with the best approximation achieved when a 2-parameter power equation was used:

$$\left(\frac{\Delta l}{l_o}\right)_{ES} = ES_{max} \cdot (1-t^{-b}), \quad t<t_{onset} \qquad (1)$$

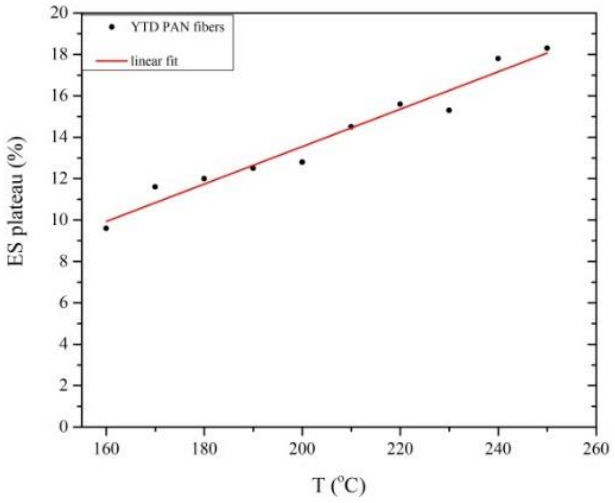

(a)

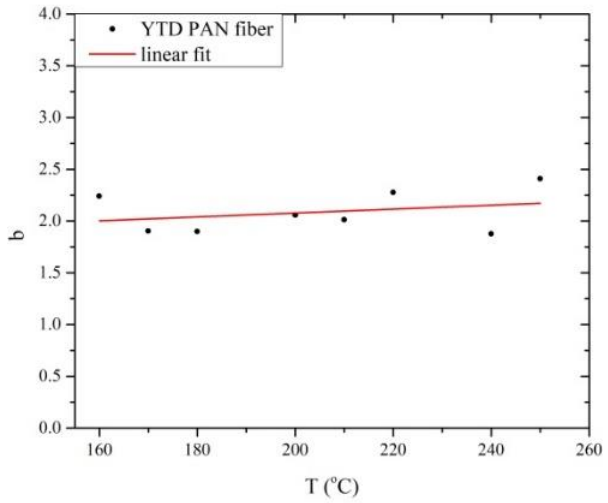

(b)

Figure 5. (a) ES plateau and (b) exponent b of equation change with stabilization temperature.

The parameters in equation (1) have distinct physical meaning: ES_{max} corresponds to the maximum-plateau value of ES, while b value corresponds to ES dependence on time. Figure 5 shows that the maximum ES value generally increases with temperature for both types of PAN fibers. This is attributed to the decrease of nitrile polar interactions, which consequently leads to decrease of the intermolecular cohesion forces, and therefore higher chain mobility. PAN has been described as polymer containing a paracrystalline and an amorphous phase [22,44]. The detailed investigation of physical changes in PAN structure during stabilization showed that the ordered phase content was minimized at 150 °C (under free shrinkage conditions) [23]. The consensus in the literature is that the intermolecular interactions are higher in the amorphous than the ordered state [44], and thus, the increase of the amorphous content seems to obstruct ES at 150 °C. The dependence of ES on time could possibly be attributed to different shrinkage rates between the amorphous and crystalline regions of PAN [1,10]. In the present study, shrinkage was varied between 10 and 20% with increase in stabilization temperature. In Figure 5 the values of parameter b are depicted. A mean b value is measured at 2.09 for YTD PAN fibers.

3.2 Contribution of Creep

In order to quantitatively describe the thermomechanical behavior of polymers, several models have been proposed that involve mechanical elements like springs and dashpots. For example, in the Burgers model the influence of the elastic, the viscoelastic, and the viscoplastic contribution are used for describing the creep behavior; the elastic terms correspond to recoverable creep and plastic to non-recoverable [45]. In the case of thermal oxidative treatment of the PAN fibers, in order to investigate if there is any recovery, the length of fibers was measured after each treatment and the result was compared to the length change. Due to lack of length recovery, it was assumed that permanent change in length occurred; hence, the creep can be described as a viscoplastic flow. Following the determination of ES, the creep was calculated by subtracting the ES from length change (Figure 6). It can be observed that PAN fibers do not behave as a linear viscoelastic material in the high stress region. Even though there are several possible approaches that could be used for investigating this non-linear creep behavior, the proposed model is shown in equation (2) [21,46]:

$$\left(\frac{\Delta l}{l_o}\right)_{creep} = A\cdot(c_T - a_T\cdot T)\cdot(a_m\cdot\sigma - c_m)\cdot t\cdot\exp\left(-\frac{E_a}{RT}\right)\cdot\exp\left(-\frac{\delta\cdot\sigma}{2k_BT}\right) \quad (2)$$

where,

A: pre- exponential factor ($sec^{-1}\cdot K^{-1}$)
T: treatment temperature (K)
t: duration of the treatment (sec)
E_a: activation energy of creep ($kJ\cdot mol^{-1}$)
a_T: slope related to temperature
c_T: constant related to temperature
R: gas constant ($8.314\ J\cdot K^{-1}\cdot mol^{-1}$)
σ: stress applied on the fibres (MPa)
δ: activation volume ($Å^3$)
k_B: Boltzmann constant ($1.381\cdot10^{-23}\ J\cdot K^{-1}$)
a_m: slope related to applied stress
c_m: constant related to applied stress

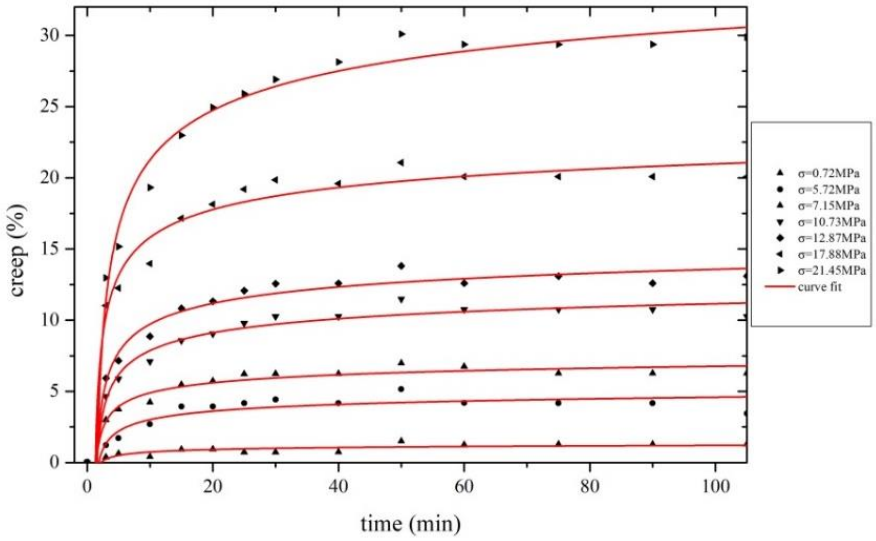

Figure 6. Creep curves for isothermal stabilization of YTD PAN fibers at various applied stress.

This expression is adapted from a similar equation that was firstly proposed for modeling the shrinkage of PAN fibers during their thermomechanical treatment and it has been derived from the Eyring model that describes the flow of solids as an activation energy- driven process [21,46].

The required stress for preventing fiber shrinkage can be obtained using equation (2), considering steady state of creep during stabilization, and for adjusting the applied tension in order to ensure that physical damage of orientation and crystallinity is prevented [23,47].

Equation (2) contains several structural parameters that should be calculated from the experimental results before its implementation; their calculation will be presented bellow.

3.2.1 Determination of creep activation volume δ

Initially, the activation volume δ can be estimated using isochronous plots of creep logarithm versus applied stress (σ) for a given temperature (**Figure 7**). In this occasion equation (3) is transformed as:

$$ln(\frac{\Delta l}{l_o})_{creep} = ln(A \cdot t) + \ln(c_T - a_T \cdot T) + \ln(a_m \cdot \sigma - c_m) - \frac{E_a}{RT} - \frac{\delta \cdot \sigma}{2kT} \quad (3)$$

In equation (3), the parameter: $[\ln(c_T - a_T \cdot T) + \ln(a_m \cdot \sigma - c_m)]$ can be considered as constant. It should be noted that creep below 5 MPa (critical value), was excluded, as the behavior changes to linear viscoelastic.

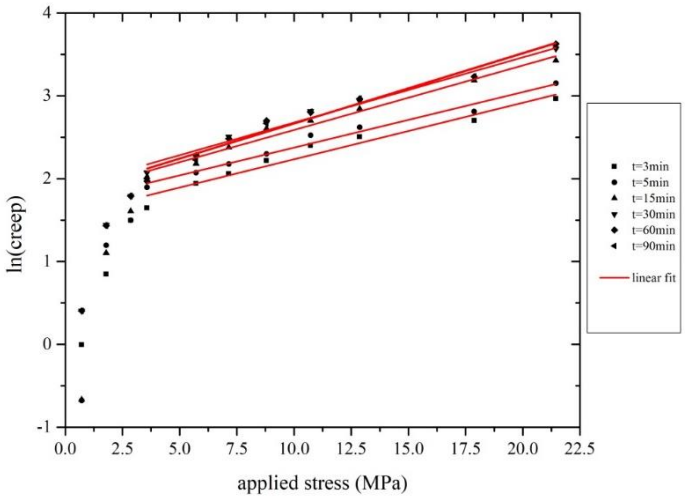

(a)

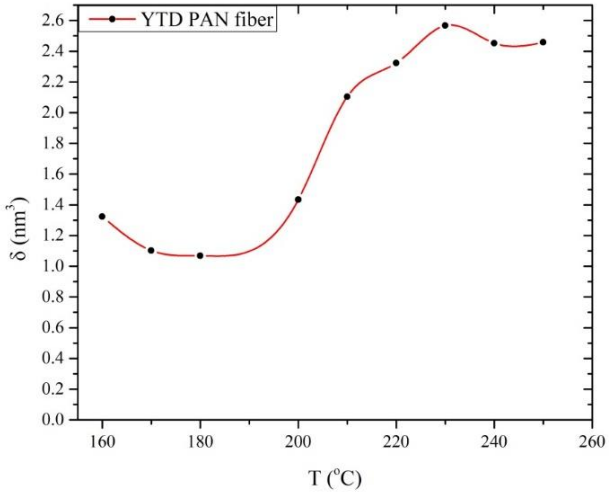

(b)

Figure 7. (a) Isochronous plot of creep logarithm vs stress during stabilization of YTD PAN fibers, (b) Dependence of creep activation volume (δ) on stabilization temperature for Fibers A and B.

The values of δ were calculated for each treatment time and temperature; for a fixed temperature δ is practically independent of treatment time. The aforementioned trend was anticipated considering the creep elongation mechanism, derived by displacement and increase in distance between basic molecular units in PAN macromolecule. The dependence of δ on temperature

is shown in **Figure 7**b. The possibility of the chemical reactions affecting the mobility is rather small. More specifically, the onset of the dehydrogenation and/ or oxidation reactions (as evidenced by the beginning of the fiber color change [21]), is several hours long. Should dehydrogenation be the case, it could have been surmised that the importance of the reactions would had increased by increasing temperature (i.e. leading to even higher δ values). This was not observed, indicating that the effect of the chemical reactions is minimal at this temperature range. The behavior of δ as a function of temperature can be traced to the change in the ordered regions of PAN: it has been proven that low-temperature treatment of the PAN fibers under stretching causes an increase of both the orientation and the size of the ordered regions (L_c) [22]. Between 150 and 170 °C the increase of L_c is steep (from 90.3 nm to 111.3 nm). Even though part of this increase is attributed to the corresponding increase of the inter-chain spacing inside the ordered regions (from about 6.14 to about 6.17 nm) [48], the values indicate that applying stress on the fibers results in enlargement of the ordered regions, which resembles to "stress-induced crystallization". It can be surmised that this increase of L_c acts as an additional obstacle to the segmental mobility that causes the small (albeit non-trivial) decrease of δ.

It is worth commenting on the already mentioned (and similar) decrease in ES plateau values (Figure 5); however, in the latter case the decrease is at somewhat different temperature (150 °C, compared to 160 °C for δ). In the literature there are reports on transitions at this temperature; Bashir [44] attributes this to the glass - rubber transition of the amorphous phase of PAN. The temperature discrepancy between the two parameters indicates that this transition is stress- sensitive: the ES plateau corresponds to "free shrinkage" conditions (and is affected by the amorphous content) and the values of δ to "under stress" conditions (and is mostly influenced by the ordered regions). It is also worth noticing that recently published TMA measurements of PAN fibers indicated to such an eventuality [41]. The aforementioned temperature discrepancy between the two parameters indicated that this transition is dependent on copolymer composition [47,49]. The decrease of δ above 220 °C could possibly be attributed to the effect of chemical reactions on fiber structure; dehydrogenation reactions create conjugated structures on the polymer backbone, leading to increased rigidity and reducing the segmental mobility [30].

3.2.2 Evaluation of Creep Activation Energy

For the calculation of activation energy, the treatment conditions should be defined, where the fibers have the same degree of creep when subjected to the same applied load. These points can be detected in the isostress plot of the creep vs. time; afterwards, they are plotted in the form of [ln(t*T) vs. (1/T)]. Then, the activation energy can be calculated from equation (4) (C representing a constant):

$$\ln\left(t\cdot\left(c_T - a_T\cdot T\right)\right) = \frac{E_a}{R}\cdot\frac{1}{T} + C \qquad (4)$$

An average value of E_a is calculated as 335 kJ/mol. This value is rather high and means that the effect of the term: [exp(-E_a/RT)] on the creep is not as important as the other parameters in eq. (2). This possibly also explains the already mentioned insensitivity of the intercept in the isochronous [ln(creep)-σ] plots (**Figure 7**a) to the temperature.

Peer-reviewed version available at Materials 2020, 13, 2749; doi:10.3390/ma13122749

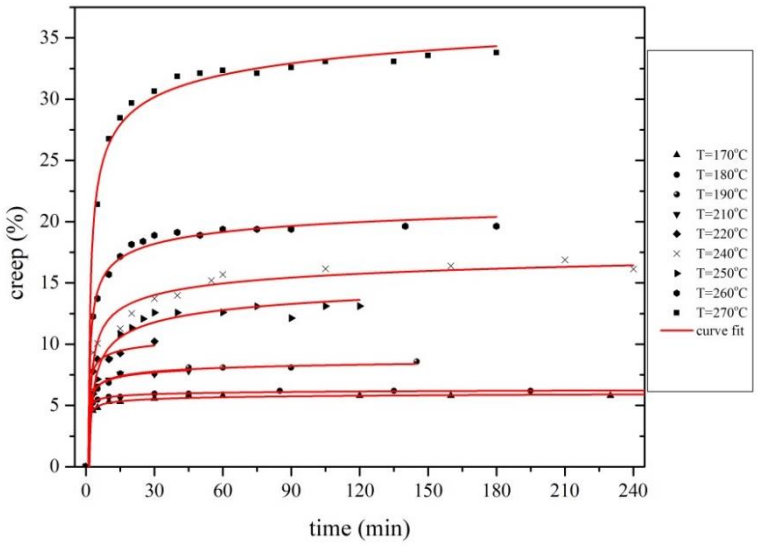

Figure 8. Creep elongation behavior during stabilization at isostress conditions at 12.87 MPa for YTD fiber.

Figure 8 shows the fitting of the proposed model with the corresponding experimental creep–time data sets; a good approximation is achieved.

3.3 Contribution of Chemical Shrinkage (CS)

The chemical shrinkage (CS) is attributed to the nitrile cyclization reaction that takes place during the thermal oxidative treatment; specifically, intra-molecular cyclization causes considerable decrease of the length of the PAN macromolecules. CS does not begin instantaneously: even at high treatment temperature there is an incubation time. The pre-heating time needed for the beginning of CS is termed cyclization onset time (t_{onset}). In the treatment region below the onset of CS the chemical reactions that take place (i.e. oxidation and / or dehydrogenation) seems that effect only marginally the length change of the PAN fibers (even though they do affect the structure of the PAN fibers). It has been found that the CS – time curves can be fitted with exponential rise to maximum equations:

$$\left(\frac{\Delta l}{l_o}\right)_{CS} = [CS]_{max}\left(1 - e^{-k \cdot t_R}\right) \qquad t > t_{onset} \qquad (5)$$

This expression can be directly linked to the nitrile cyclization and corresponds to first order reaction kinetics (with respect to the concentration of the nitrile groups) [30], which was also confirmed for the PAN fibers investigated (**Figure 9**). Parameter $[CS]_{max}$ in eq. (5) corresponds to the maximum extent of CS at a certain temperature, and it is possible to be used in the estimation of the intra- and inter-molecular nitrile cyclization ratio.

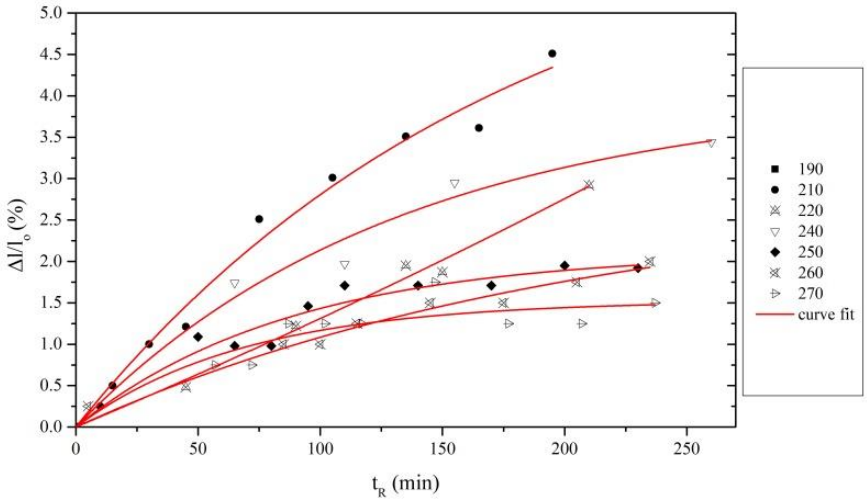

Figure 9. Chemical Shrinkage fitting using stabilization model versus reaction time t_R.

The parameter k is corresponding to nitrile cyclization rate and can be used for determining the kinetics of the cyclization reaction. For YTD PAN fibers the cyclization activation energy was calculated at 131.6 kJ/mol. As reported in the literature, cyclization E_a is in the region of 100-150 kJ/mol, while any deviation could be attributed to the different comonomers used in PAN various copolymers [30,50]. The CS plateau increased gradually from 8% up to 14%, indicating that cyclization proceeds mainly through inter-molecular reactions [29,30].

$$ln(t_{onset}) = \frac{E_a}{R} \times \frac{1}{T} - lnA_o \quad (5)$$

The values of E_a and k_o were measured for YTD PAN fibers at 140.3 kJ/mol and 0.476 sec^{-1}.

The final aspect of the model is t_{onset}. Figure 10 shows that t_{onset} has an Arrhenius-type dependency on temperature. This parameter actually represents the treatment conditions, where the nitrile cyclization reactions are initiated; i.e. the time were the conversion α is zero and the derivative of conversion is $(d\alpha/dt)>0$.

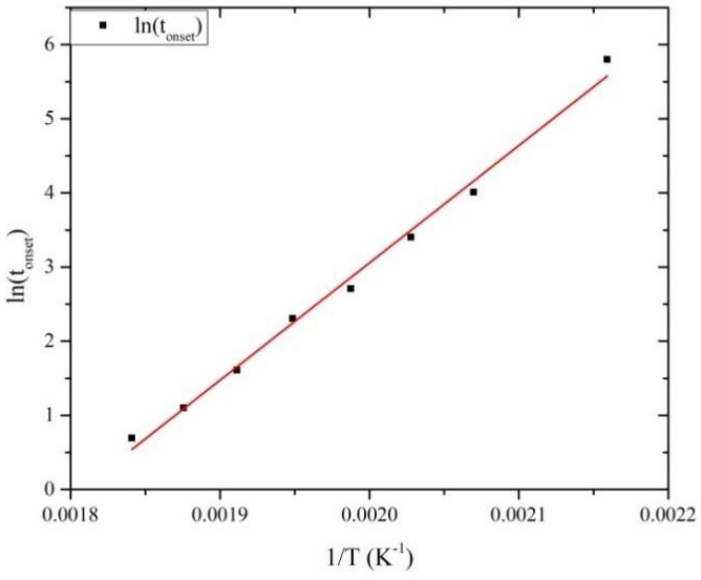

Figure 10. Arrhenius plot of t_{onset} versus stabilization temperature.

3.4 Fourier Transform Infrared Spectroscopy

Figure 11 shows the FTIR spectra of several oxidatively treated PAN fibers. According to literature, applied load does not affect chemical structure of treated fibers [21,30], and thus stabilized fibers were characterized independently of the applied load.

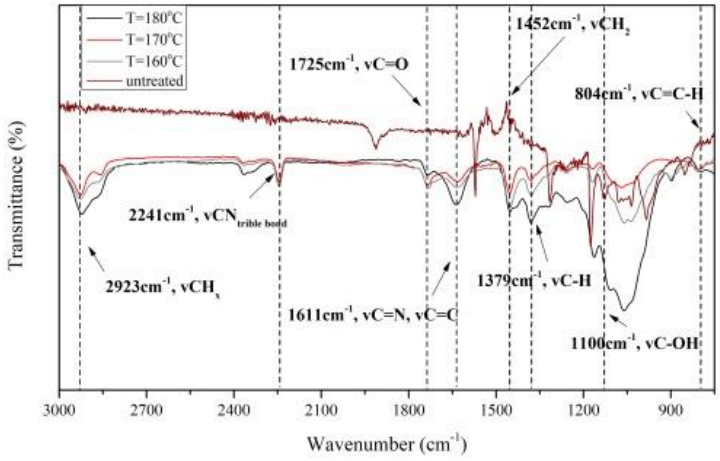

(a)

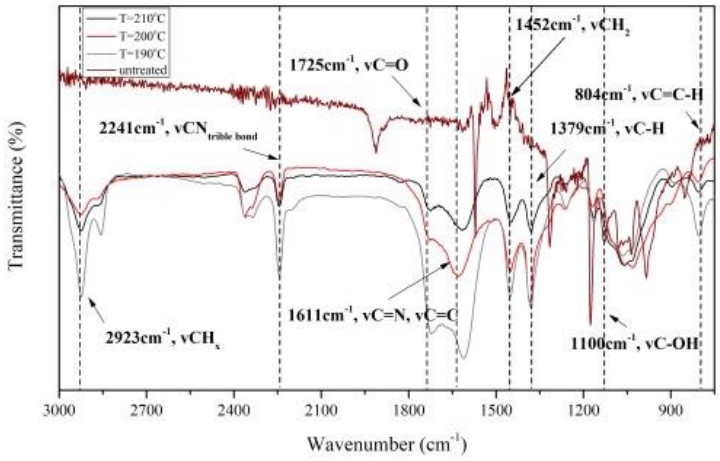

(b)

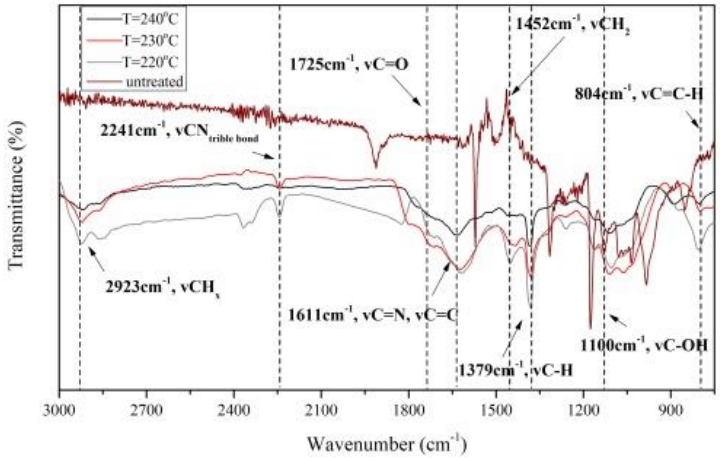

(c)

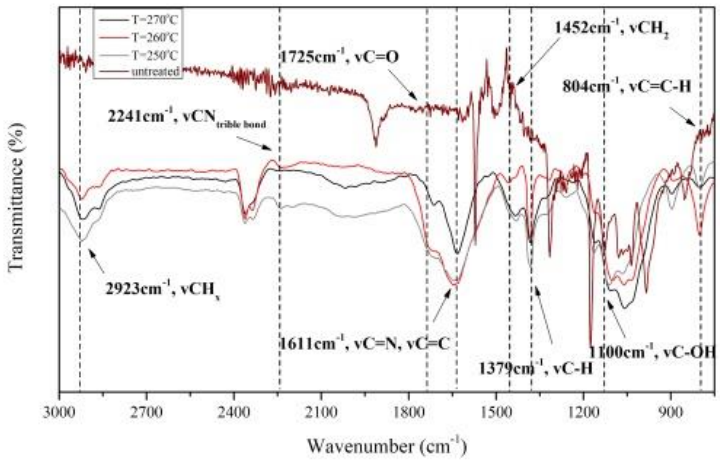

(d)

Figure 11. FT-IR spectra of virgin and stabilized fibers in range of (a) 160-180°C, (b) 190-210°C, (c) 220-240°C, (d) 250-270°C. In each case, treatment duration was 4h.

It can be seen that, by increasing intensity of treatment (either the temperature or the duration), the intensity of peaks at 2940 cm^{-1} and 2240 cm^{-1} (attributed to the methylene and nitrile groups, respectively) decrease, due to dehydrogenation and cyclization reactions, respectively. Peaks at around 1740 cm^{-1} and 1600 cm^{-1} attributed to the carbonyl and the conjugated double bonds are progressively formed as expected, with simultaneous decrease of the methylene groups (which can be better observed from the peak at 1446 cm^{-1} rather than 2924 cm^{-1}) [7,8,11,13,16,21,23,28,51,52]. By comparing the spectra at 150 °C and 200 °C, a higher reduction of methylene groups than of the -C≡N groups is observed, indicating that in the latter case dehydrogenation progressed to higher degree. The peaks at 1382 cm^{-1} and 1219 cm^{-1} are mainly related to C−H, which should not be detected in thermally stabilized PAN fibers due to dehydrogenation.

Table 1. Major peaks to be characterized in FTIR spectra.

Wavenumber (cm^{-1})	**2924**	**2239**	**2107**	**1725**	**1658**	**1583**	**1446**	**1357 & 1262**	**1163**	**1097 & 1064**	**804**
Bonds	CH_x	C≡N	C=NH	C=O	C=C asymmetral vibration	C=C, C=N	Tensile vibration CH_2	C-H vibration	C-O	C-OH	=C-H
Major FT-IR peaks before stabilization	√	√	√	√	×	×	√	×	√	×	×
Major FT-IR peaks after stabilization	√	↓	√	↑	√	√	↓	√	√	√	√

The peaks in the FT-IR spectra are summarized in **Table 1**. Due to the use to KBr pellet technique, several peaks can be used for quantitative analysis, in order to monitor the reaction progress. Cyclization index (CI) and nitrile to methylene ratio (r_{nm}) are used:

$$CI = \frac{I_c}{I_C + I_n} \quad (6)$$

$$r_{nm} = \frac{\left(\frac{I_n}{I_m}\right)_{treated}}{\left(\frac{I_n}{I_m}\right)_{pristine}} \quad (7)$$

where I_c, I_n and I_m are the intensities of peaks at 1,600 (conjugated double bonds), 2,240 cm^{-1} (nitrile groups) and 2,940 cm^{-1} (methylene groups), respectively.

Using **Table 1** to investigate the chemical transformations during the treatment of the fibers at different temperatures, the FT-IR spectra in **Figure 11** showed a progressive reduction of nitrile bonds, along with a reduction of the methylene groups of the macromolecular backbone. Simultaneously, as the temperature is elevated, the formation of C=N and C=C conjugated double bonds progresses, as observed by the growth of the peak in the region of $1600cm^{-1}$, along with the carbonyl groups (C=O) at $1730cm^{-1}$, and of the C-OH units at $1100cm^{-1}$, which were formed due to the oxidative reactions during the thermal stabilization of PAN fibers; moreover, the appearance of a peak at approximately $800cm^{-1}$ can be attributed to the C=C-H footprint of stabilization process at $806cm^{-1}$. In order to quantifically evaluate the stabilization, equations (6) and (7) are used, and the results are summarized in Table 2.

Table 2. Values of treatment indexes r_{nm} and CI calculated from FTIR spectra via Lambert-Beer Law.

Stabilization Temperature (°C)	CI	r_{nm}	Cyclization	Dehydrogenation
160	0.43	2.50	low	High
170	0.44	1.91	low	Medium
190	0.65	2.24	mid	High
200	0.64	2.97	mid	High
210	0.64	1.84	mid	High
230	0.83	0.99	high	High
240	0.91	0.74	high	High
250	0.94	0.44	high	High
260	0.97	0.41	high	High
270	0.98	0.11	high	High

Oxidative treatment at low temperatures (i.e. 160 and 170 °C) showed low cyclization yield. However, the appearance of a peak at 1640 cm^{-1} indicates the formation of conjugated double bond structures. The values of r_{nm} indicate that these structures are the result of the dehydrogenation reactions. By increasing the treatment temperature above 190°C, the value of CI increased due to extensive cyclization. Generally, when the treatment is in the region 200-210°C the values of r_{nm} exceed 1, indicating that both dehydrogenation and cyclization reactions contribute to ladder polymer formation. The gradual decrease of the r_{nm} values in the temperature region 200-270°C indicates that increasing contribution of the cyclization reactions to the formation of conjugated double bond structures as the treatment temperature increases. Above 240°C, CI reaches high values indicating that cyclization reactions are almost complete. During high-temperature stabilization (i.e. between 250-270°C) a large methylene peak, a weak peak of carboxyl groups at $1730cm^{-1}$, and a peak for the conjugated double bonds at 1630 cm^{-1} were detected. As it is implied, in this temperature region oxidation occurs in a low extend, probably due to the slow diffusion of oxygen in the radial direction of the fiber; moreover, oxygen may initiate an alternative reaction pathway towards the formation of active centers for cyclization, thus the preferential initiation of the cyclization reaction acts competitively to the oxidation reactions [13,22,23,36].

3.5 Raman spectroscopy

In order to investigate the evolution of the microstructure and the formation of ordered graphitic planes, Raman spectroscopy was performed on Fiber B specimens. These fibers were treated isothermally at 160 °C to 270 °C for 4h duration under 300g of applied force. The samples were fixed on a microscope glass slide in order to have the best focus on the analysis point. It was possible to detect the Raman signal only in samples treated at temperatures above 200 °C. In these samples, an extremely low intensity of signal in the 2D region was observed. In addition, the shape of the signal did not show a peculiar behavior and the introduced measure uncertainty by the baseline correction

procedure was high. For these reasons the measurement was performed in static scan mode with center at 1550 cm^{-1}. Laser power started from 0.06 mW, and reached 3 mW or 50% of the maximum available power of 6 mW.

As can be observed in Figure 12 (a), untreated and thermally treated samples in the range 160-200 °C presented a similar spectroscopic behavior. To avoid CCD sensor saturation, all the samples were measured at low power of the laser source, from 0.006 mW to 0.06 mW. All the samples showed an intense fluorescent signal without any trace of Raman activity. By visual examination of the fibers, their color was observed to progressively change from a white for the untreated fiber towards progressively darker colors as the treatment temperature increases. The lack of any Raman activity indicates the absence of cyclized structures, but the strong fluorescent signal can be attributed to the presence of non-cyclized organic compounds.

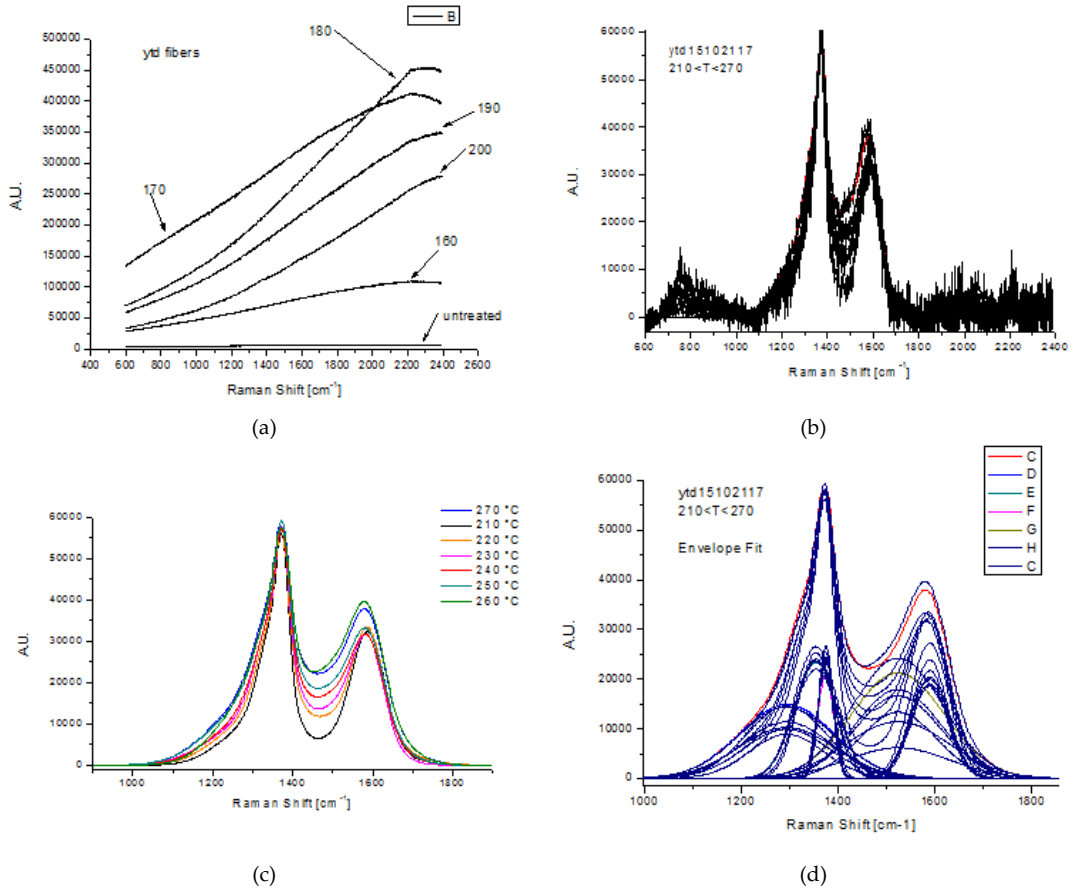

Figure 12. Raman spectra of thermally treated fibers (a) isothermally treated at temperature between 160-200°C. Isothermally treated at temperature between 210-270°C (b) after Baseline correction and subtraction (c) after noise reduction and D-peak normalization (d) after fitting the entire spectrum.

The Raman spectra of thermal treated samples in the region of 210-270°C are presented in Figure 12(b). Fibers treated at temperatures above 200 °C exhibited Raman activity similar to that of the stabilized PAN fibers, an indirect indication of oxidation progress [11,23,33]. In this case, the presence of Raman activity in both the D and G regions can be seen (along with a strong fluorescent signal). These fibers contain ladder polymer structures and have shiny black color; thus, a greater laser power could be applied to analyze the samples (in order to avoid the saturation of CCD sensors). The laser source power ranged from 10 to 50 % of maximum potential. The Raman spectra of Figure 12(b) were normalized on the D peak at 1372cm^{-1} and cleared by noise reduction; the final results are presented in Figure 12(c). For further quantitative analysis of structural transformations during the treatment, the curves of the Raman spectra stabilized fibers were fitted using a number of peaks that describe the entire signal, as seen in Figure 12 (d)).

Peer-reviewed version available at Materials 2020, 13, 2749; doi:10.3390/ma13122749

The initial PAN fibers and those treated below 200°C are Raman inactive. A different trend is presented at higher temperatures, where cyclization seems to have altered the structure of the fibers [53]. Looking the peak fitting in Figure 12(d), it can be clearly seen that the D and G regions are fitted with five different Gaussian components, three for the D peak and two for the G peak. The D peak is described by two components centered at 1354cm^{-1} and 1375cm^{-1}, respectively, that exhibit a small intensity variation with the treatment changes of the treatment temperature; the third component (around 1290cm^{-1}) shows higher variation. The G peak has a component around 1590cm^{-1} not significantly affected by treatment temperature and a second component at 1520cm^{-1} that increases as the treatment temperature increase [49,54,55]. In general, as temperature is increased the ratio I_D/I_G tends to decrease, due to the enrichment of the fibers with turbostatic graphite structures (i.e. the G peak), due to the effect of cyclization and aromatization reactions, and thus stabilization treatment at elevated temperature is proved to be more effective [56-58]. Amplitude, Center and width for each component are reported Appendix A (in Table A.1. Raman Data Tables).

3.6 Thermal Analysis

The results of the thermal analysis in air atmosphere are presented in Appendix A (Figure A.2) and are summarized in Table 3.

Table 3 Results of thermal analysis of oxidatively stabilized PAN fibers.

Stabilization Temperature (°C)	ΔH_{total} (J/g)	Stabilization Index (SI)
---	276.6	0.0%
160	230.3	16.7%
170	118.6	57.1%
180	118.4	57.2%
190	96.6	65.1%
200	112.4	59.4%
210	125.7	54.6%
220	22.6	91.8%
230	12.6	95.4%
240	4.3	98.4%
250	4.5	98.4%
260	10.8	96.1%
270	19.1	93.1%

The results of the thermal analysis in nitrogen atmosphere are presented in Appendix A (Figure A.3). The measured heat released is due to the exothermic, intra- and inter-molecular cyclization, the only occurring action under such conditions (since dehydration dehydrogenation and oxidation reactions are triggered by the presence of O_2) [1,6,11,13,33,47,59,60].Confirmation that only a single event occurs is obtained by TGA (where a bending point is observed in DTG), while the DSC exotherm is accompanied by minor weight loss, a behavior characteristic of cyclization reactions [28]. The results of this analysis are presented in Table 4.

Table 4. Results of thermal analysis of stabilized PAN fibers in inert atmosphere.

Stabilization Temperature (°C)	$\Delta H_{cyclization}$ (J/g)	Cyclization Index (CI)
---	184	---
160	174.9	4.9%
170	143.9	21.8%
180	100.8	45.2%
190	66.2	64.0%

200	62.9	65.8%
210	54.5	70.4%
220	21.1	88.5%
230	20.7	88.8%
240	6.9	96.3%
250	0.4	99.8%
260	5.5	97.0%
270	7	96.2%

3.7 Comparison of the cyclization yield derived from DSC, FT-IR and chemical shrinkage model

The enthalpy measured via DSC can be used for determining the progress of the cyclization through the Cyclization Index (CI) [40]; the results obtained by DSC can be compared with those acquired from the FT-IR measurements and with those derived from the model of chemical shrinkage [1,8,28,33,49]. The results of the different approximations are summarized in Figure 13. It is clear that the three methods yield similar results for the progress of the cyclization. As a general trend, DSC-derived CI tend to have somewhat higher values. This is probably attributable to the limitations of DSC as a measurement method; namely, due to the definite heating rate, part of the heat evolved at high temperatures diffuses and is not accounted for, i.e. the residual exotherm is underestimated. The differences between the CI values estimated from the chemical shrinkage model and from the FTIR decrease as the treatment temperature increases. This effect could be attributed to the effect of the dehydrogenation reactions. Namely, the CI derived from the chemical shrinkage takes into account only the effect of the nitrile cyclization reactions, whereas the CI from FTIR accounts for all conjugated structures (independent of their origin). In seems that the fibers treated at 230 °C contain in their structure a considerable amount of linear conjugated structures, which is the end product of dehydrogenation reactions; gradually, as the treatment temperature increases, the CI values increase and their differences diminish. The latter phenomenon is a clear indication for the domination of the nitrile cyclization reactions and the concurrent marginalization of the backbone dehydrogenation reactions.

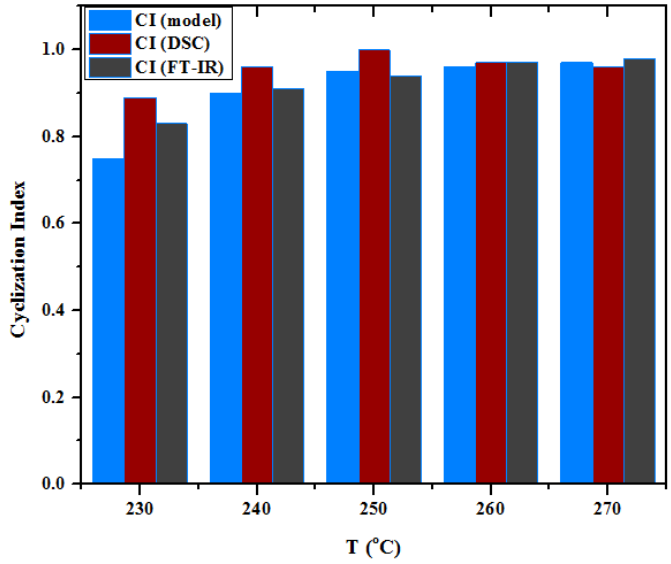

Figure 13. Comparison of estimations for the cyclization progress derived from three different methods: chemical shrinkage model, DSC and FTIR.

3.8 Investigation of cross-section circularity after thermal treatment

The cross-section area of treated PAN fibers at 160, 210, 230, and 260◦C (that were observed by optical microscopy) was pointed out that the chance of cross-sectional shape alternation was almost

Peer-reviewed version available at *Materials* **2020**, *13*, 2749; doi:10.3390/ma13122749

1:1, so that when a monofilament was observed, the possibility to be of circular area is almost the same as to obtain a different shape (Figure 14). In order to prove the effect of cross-sectional shape alternation in the estimation of the total fiber cross-sectional area, a thorough study of the stabilized fibers surface was conducted. In each case, three characteristic areas were measured, while at least 40 monofilaments were measured for initial and treated fibers, considering the features of radius and area in order to obtain statistically correct results. A mean value was estimated along with the standard deviation, while the measurements in case of deformed fibers were obtained using *ImageJ*,. An equal cyclic radius was estimated-ECR (or equivalently the diameter, ECD) [1], along with a mean value, and the standard deviation were determined. The results are summarized in Table 5 below.

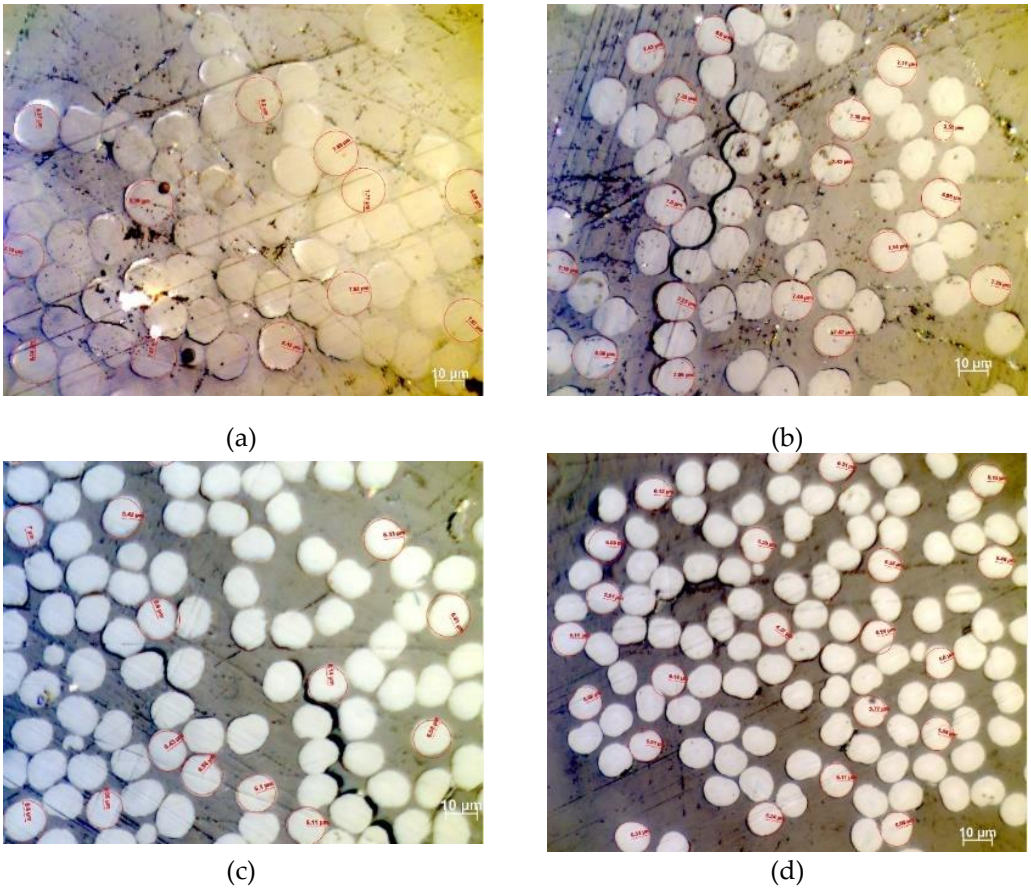

Figure 14. Optical Microscopy of stabilized PAN fibers at temperatures of (a) 160°C, (b) 210°C, (c) 230°C, and (d) 260°C.

Table 5. Synopsis of alternation of PAN cross-sectional area investigation results through OM.

Stabilization Temperature (°C)	**160**		**210**		**230**		**260**	
Software	OM	ImageJ	OM	ImageJ	OM	ImageJ	OM	ImageJ
Mean Radius (μm)	7.76	7.35	7.22	6.90	6.43	6.18	6.01	5.69
Standard Deviation	0.48	0.34	0.30	0.33	0.31	0.30	0.29	0.16
Mean monofilament area (μm²)	188.9	169.8	163.6	149.8	129.8	120.3	113.5	101.6
Standard Deviation of Monofilament Area	0.71	15.94	0.29	14.28	0.31	11.72	0.26	5.71

As presented in Table 5, the cross-section of deformed fibers exhibits a decreasing trend with temperature. However, estimation of mean area permitted the estimation of the importance of cross-

section variation . For all cases, the variation in PAN monofilament radius and the derived total area was in the limits of standard deviation, and more specifically approaching the lower limit.

4. Conclusions

A comprehensive model for monitoring the stabilization process of PAN fibers was introduced, utilized to support a methodology for controlling the process. Following extensive characterization and mapping of the stabilization process, application of this model contributes to avoid the consideration of complex chemical reactions; this approach could be used for improving stabilization time-and energy-efficiency. It was confirmed that cyclization is described by first order reaction kinetics. Simultaneously, cyclization yield is can be accurately calculated at high temperature via a simple relation, wherein macroscopic change in length was involved; the results were further confirmed by FT-IR and DSC-derived reaction yields. The knowledge of length variation in different stabilization conditions through the application of this model could permit the optimization of the process. Moreover, there is the potential to optimize mechanical properties after carbonization by achieving controlled of cyclization yield (via proper stabilization variables control). A further gain is the applicability of this model for oxidative stabilization at both batch and continuous processing plants, as the employed values of fiber length change, temperature, tension, and residence time are taken into consideration. Finally, considering a multistage process, this model could be applied both during the initial stages (to determine parameters to control elongation of PAN fibers), as well as during main stabilization (as the kinetic parameters of cyclization from chemical shrinkage can help minimize energy consumption and time).

Using FTIR and Raman spectroscopy, it is feasible to study the evolution of chemical structure and ladder polymer formation, using aromatic index, G-peak activity, and fiber shrinkage to enhance understanding of the processing parameters. Thermal analysis provided additional insight related to the progress of cyclization and the overall progress of cyclization reaction.It was shown by FTIR analysis that dehydrogenation is the basic reaction that occurs below 200°C, while both cyclization and oxidation reactions are important at higher temperatures. This was also confirmed by DSC and Raman. Raman also confirmed structural transformation of the linear PAN molecule to ladder polymer, where the formation of graphite-like sp^2 planes start to appear as a result of stabilization at temperatures above 200°C. Thus, in order to obtain a sufficiently stabilized PAN fiber, the fiber should be treated at temperature higher than 200°C. These results come to an agreement with previous FT-IR results, while the introduced model provided similar results, i.e. that stabilization using two or more different temperature stages should be used in order to optimize the chemical structure by controlling yield of oxidation, dehydrogenation and cyclization reactions. Consequently, the effectiveness of stabilization process could be increased. The cross-section investigation via Optical Microscopy was used to estimate the area and the circulatity of thermal treated PAN fibers and it was concluded that thermal treatment had minor effect in fibers microstructure.

Author Contributions: Conceptualization, S. S., D.A.D. and G.K.; Methodology, S.S., D.A.D. and G.K.; Formal Analysis, S.S., D.A.D. and G.K.; Investigation, S.S. and G.K.; Resources, C.A.C.; Data Curation, D.A.D. and G.K.; Writing-Original Draft Preparation, C.A.C., D.A.D., G.K., and S.S.; Writing-Review & Editing, C.A.C., D.A.D., G.K., and S.S.; Visualization, C.A.C., D.A.D. and G.K.; Supervision, C.A.C., D.A.D., S.S., and G.K.; Project Administration, C.A.C., D.A.D.; Funding Acquisition, C.A.C., D.A.D.

Funding: This work was supported by HORIZON 2020 Collaborative project "SMARTFAN". The abbreviation "SMARTFAN" stands for Smart by Design and Intelligent by Architecture for turbine blade fan and structural components systems" (Grant agreement no.: 760779).

Conflicts of Interest: The authors declare no conflict of interest.

Appendix A

A.1. Raman Data Tables

ytd15102117_210

Area	Center	Width	Shape	ID/IG
1.714E+06	1293.353	76.866	Gaussian	1.14
2.322E+06	1354.051	36.573	Gaussian	
9.812E+05	1374.569	14.640	Gaussian	
1.643E+06	1523.361	106.078	Gaussian	
2.750E+06	1589.261	40.364	Gaussian	
ytd15102117_220				
Area	Center	Width	Shape	ID/IG
2.184E+06	1293.353	87.784	Gaussian	1.04
2.374E+06	1354.051	39.445	Gaussian	
9.444E+05	1374.569	14.738	Gaussian	
3.052E+06	1523.361	106.417	Gaussian	
2.227E+06	1589.261	37.194	Gaussian	
ytd15102117_230				
Area	Center	Width	Shape	ID/IG
2.561E+06	1293.353	99.535	Gaussian	1.35
2.896E+06	1354.051	43.540	Gaussian	
9.155E+05	1374.569	14.965	Gaussian	
2.656E+06	1523.361	79.408	Gaussian	
2.062E+06	1589.261	37.930	Gaussian	
ytd15102117_240				
Area	Center	Width	Shape	ID/IG
2.648E+06	1293.353	92.829	Gaussian	1.15
2.662E+06	1354.051	44.313	Gaussian	
9.778E+05	1374.569	16.475	Gaussian	
3.672E+06	1523.361	88.085	Gaussian	
1.772E+06	1589.261	37.850	Gaussian	
ytd15102117_250				
Area	Center	Width	Shape	ID/IG
3.537E+06	1293.353	98.379	Gaussian	1.21
2.593E+06	1354.051	44.092	Gaussian	
9.361E+05	1374.569	15.943	Gaussian	
3.965E+06	1523.361	88.573	Gaussian	
1.866E+06	1589.261	39.126	Gaussian	
ytd15102117_260				
Area	Center	Width	Shape	ID/IG
3.034E+06	1293.353	83.041	Gaussian	0.86
2.503E+06	1354.051	45.529	Gaussian	
1.018E+06	1374.569	18.630	Gaussian	
5.655E+06	1523.361	93.225	Gaussian	
1.961E+06	1589.261	39.163	Gaussian	
ytd15102117_270				
Area	Center	Width	Shape	ID/IG
3.650E+06	1293.354	97.955	Gaussian	1.00
2.638E+06	1354.051	45.256	Gaussian	
8.770E+05	1374.569	16.601	Gaussian	
5.119E+06	1523.361	96.119	Gaussian	

2.049E+06	1589.261	40.142	Gaussian

A.2. DSC-TGA-DTG analysis of PAN fibers stabilized (a) 160 °C, (b) 170 °C, (c) 180 °C, (d) 190 °C, (e) 200 °C, (f) 210 °C, (g) 220 °C, (h) 230 °C, (i) 240 °C, (j) 250 °C, (k) 260 °C, (l) 270 °C, (m) untreated in air atmosphere.

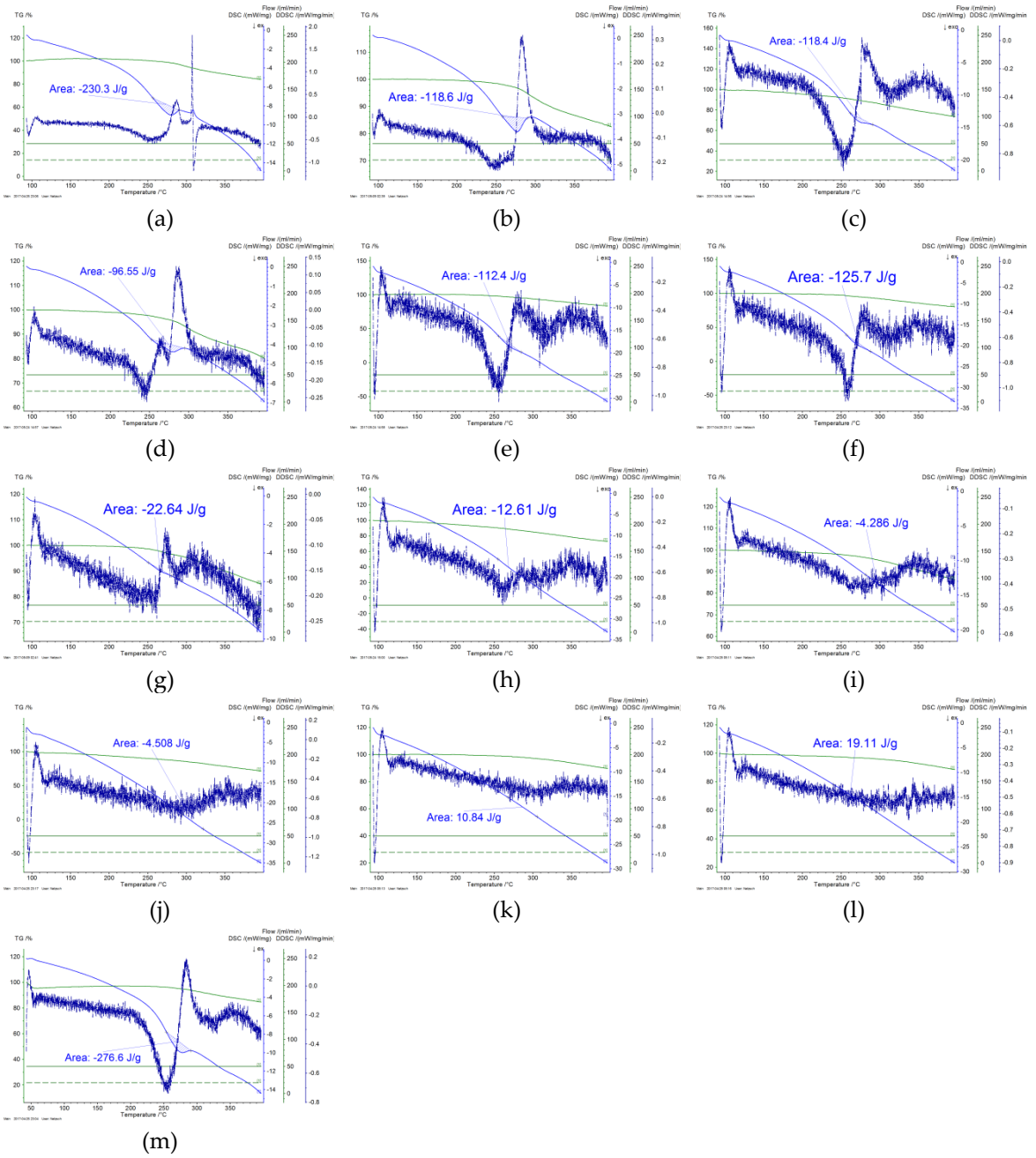

A.3. DSC-TGA-DTG thermal analysis of stabilized PAN fibers at (a) 160 °C, (b) 170 °C, (c) 180 °C, (d) 190 °C, (e) 200 °C, (f) 210 °C, (g) 220 °C, (h) 230 °C, (i) 240 °C, (j) 250 °C, (k) 260 °C, (l) 270 °C (m) untreated, tested in inert N_2 atmosphere.

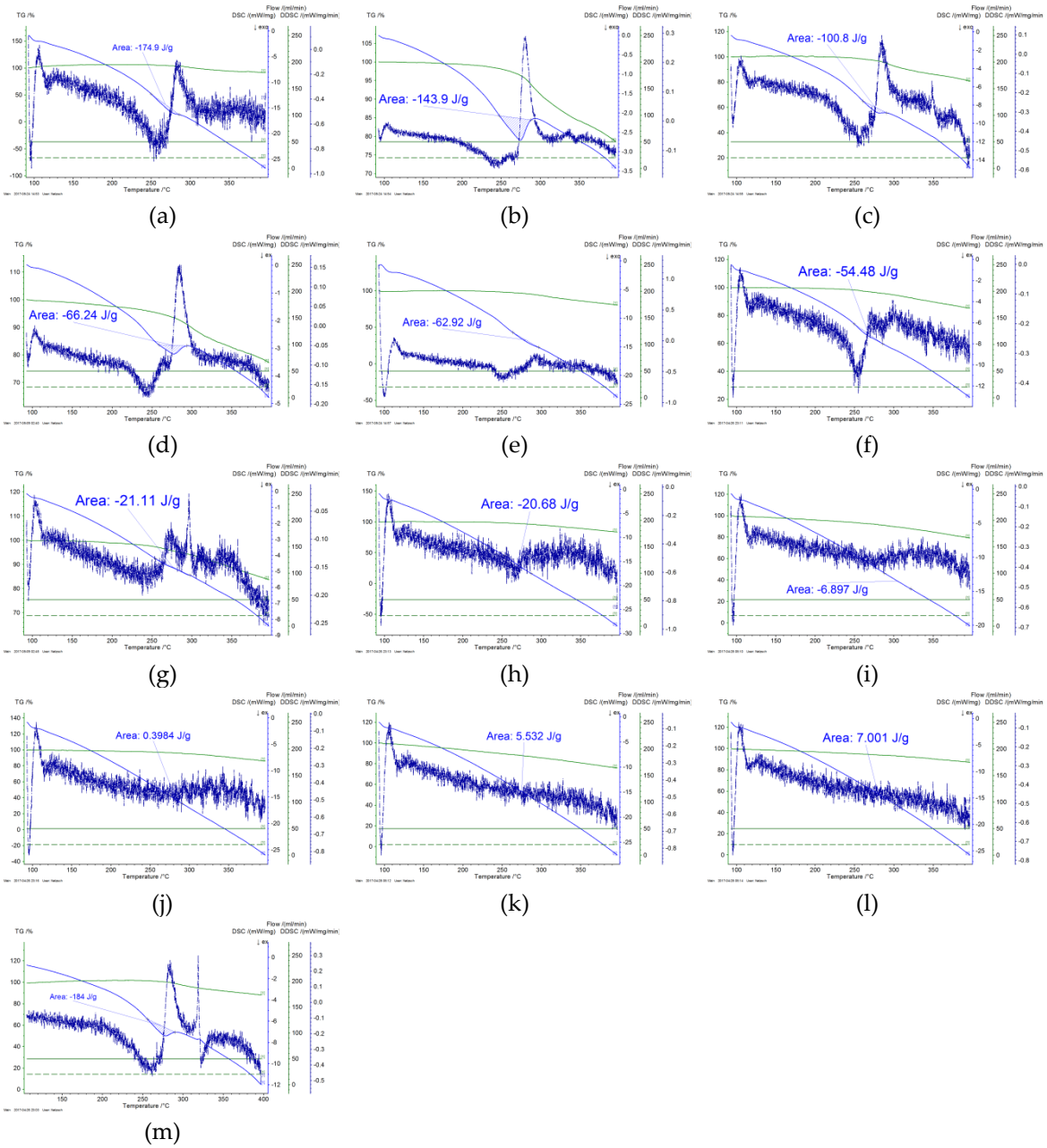

References

1. Taylor, M.P. Temperature and Strain Controlled Optimization of Stabilization of Polyacrylonitrile Precursor Fibers. University of Kentucky, Lexington, 2012.
2. Konstantopoulos, G.; Koumoulos, E.P.; Charitidis, C.A. Classification of mechanism of reinforcement in the fiber-matrix interface: Application of Machine Learning on nanoindentation data. *Materials & Design* **2020**, *192*, 108705, doi:10.1016/j.matdes.2020.108705.
3. Koumoulos, E.; Konstantopoulos, G.; Charitidis, C. Applying Machine Learning to Nanoindentation Data of (Nano-) Enhanced Composites. *Fibers* **2020**, *8*, 3, doi:https://doi.org/10.3390/fib8010003.
4. Park, S.; Yoo, S.H.; Kang, H.R.; Jo, S.M.; Joh, H.I.; Lee, S. Comprehensive stabilization mechanism of electron-beam irradiated polyacrylonitrile fibers to shorten the conventional thermal treatment. *Sci Rep* **2016**, *6*, 27330, doi:10.1038/srep27330.

5. Kim, S.-Y.; Lee, S.; Park, S.; Jo, S.M.; Lee, H.-S.; Joh, H.-I. Continuous and rapid stabilization of polyacrylonitrile fiber bundles assisted by atmospheric pressure plasma for fabricating large-tow carbon fibers. *Carbon* **2015**, *94*, 412-416, doi:10.1016/j.carbon.2015.07.012.
6. Cipriani, E.; Zanetti, M.; Bracco, P.; Brunella, V.; Luda, M.P.; Costa, L. Crosslinking and carbonization processes in PAN films and nanofibers. *Polymer Degradation and Stability* **2016**, *123*, 178-188, doi:10.1016/j.polymdegradstab.2015.11.008.
7. Xue, Y.; Liu, J.; Liang, J. Correlative study of critical reactions in polyacrylonitrile based carbon fiber precursors during thermal-oxidative stabilization. *Polymer Degradation and Stability* **2013**, *98*, 219-229, doi:10.1016/j.polymdegradstab.2012.10.018.
8. Shin, H.K.; Park, M.; Kim, H.-Y.; Park, S.-J. An overview of new oxidation methods for polyacrylonitrile-based carbon fibers. *Carbon letters* **2015**, *16*, 11-18, doi:10.5714/cl.2015.16.1.011.
9. Morris, E.A.; Weisenberger, M.C.; Abdallah, M.G.; Vautard, F.; Grappe, H.; Ozcan, S.; Paulauskas, F.L.; Eberle, C.; Jackson, D.; Mecham, S.J., et al. High performance carbon fibers from very high molecular weight polyacrylonitrile precursors. *Carbon* **2016**, *101*, 245-252, doi:10.1016/j.carbon.2016.01.104.
10. Liu, W.; Wang, M.; Xing, Z.; Qi, Y.; Wu, G. Radiation-induced crosslinking of polyacrylonitrile fibers and the subsequent regulative effect on the preoxidation process. *Radiation Physics and Chemistry* **2012**, *81*, 622-627, doi:10.1016/j.radphyschem.2012.02.029.
11. Rahaman, M.S.A.; Ismail, A.F.; Mustafa, A. A review of heat treatment on polyacrylonitrile fiber. *Polymer Degradation and Stability* **2007**, *92*, 1421-1432, doi:10.1016/j.polymdegradstab.2007.03.023.
12. Zhao, W.; Lu, Y.; Wang, J.; Chen, Q.; Zhou, L.; Jiang, J.; Chen, L. Improving crosslinking of stabilized polyacrylonitrile fibers and mechanical properties of carbon fibers by irradiating with γ-ray. *Polymer Degradation and Stability* **2016**, *133*, 16-26, doi:10.1016/j.polymdegradstab.2016.07.018.
13. Nunna, S.; Naebe, M.; Hameed, N.; Creighton, C.; Naghashian, S.; Jennings, M.J.; Atkiss, S.; Setty, M.; Fox, B.L. Investigation of progress of reactions and evolution of radial heterogeneity in the initial stage of thermal stabilization of PAN precursor fibres. *Polymer Degradation and Stability* **2016**, *125*, 105-114, doi:10.1016/j.polymdegradstab.2016.01.008.
14. Goulis, P.; Konstantopoulos, G.; Kartsonakis, I.A.; Mpalias, K.; Anagnou, S.; Dragatogiannis, D.; Charitidis, C.A. Thermal Treatment of Melt-Spun Fibers Based on High Density PolyEthylene and Lignin. *C* **2017**, *3*, 35, doi:10.3390/c3040035.
15. Goulis, P.; Kartsonakis, I.A.; Konstantopoulos, G.; Charitidis, C.A. Synthesis and Processing of Melt Spun Materials from Esterified Lignin with Lactic Acid. *Applied Sciences* **2019**, *9*, 5361, doi:10.3390/app9245361.
16. Santhana Krishnan, G.; Thomas, P.; Naveen, S.; Murali, N. Molecular and thermal studies of carbon fiber precursor polymers with low thermal-oxidative stabilization characteristics. *Journal of Applied Polymer Science* **2018**, *135*, 46381, doi:10.1002/app.46381.
17. Liu, Y.; Kumar, S. Recent Progress in Fabrication, Structure, and Properties of Carbon Fibers. *Polymer Reviews* **2012**, *52*, 234-258, doi:10.1080/15583724.2012.705410.
18. Hiremath, N.; Mays, J.; Bhat, G. Recent Developments in Carbon Fibers and Carbon Nanotube-Based Fibers: A Review. *Polymer Reviews* **2016**, *57*, 339-368, doi:10.1080/15583724.2016.1169546.
19. Huang, X. Fabrication and Properties of Carbon Fibers. *Materials* **2009**, *2*, 2369-2403, doi:10.3390/ma2042369.
20. Gilbert, M. *Brydson's Plastics Materials*, 8th ed.; Payne, E., Ed. Matthew Deans: Ed. Oxford, United Kingdom, 2017.

21. Soulis, S.; Simitzis, J. Thermomechanical behaviour of poly[acrylonitrile-co-(methyl acrylate)] fibres oxidatively treated at temperatures up to 180 °C. *Polymer International* **2005**, *54*, 1474-1483, doi:10.1002/pi.1871.
22. Sabet, E.N.; Nourpanah, P.; Arbab, S. Quantitative analysis of entropic stress effect on the structural rearrangement during pre-stabilization of PAN precursor fibers. *Polymer* **2016**, *90*, 138-146, doi:10.1016/j.polymer.2016.03.001.
23. Donnet, J.-B. *Carbon Fibers*, 3rd ed.; CRC Press: 1998.
24. Mathur, R.B.; Bahl, O.P.; Mittal, J. A new approach to thermal stabilisation of PAN fibres. *Carbon* **1992**, *30*, 657-663, doi:10.1016/0008-6223(92)90185-y.
25. Lee, S.-H.; Kim, J.-H.; Ku, B.-C.; Kim, J.-K.; Chung, Y.-S. Effect of Process Condition on Tensile Properties of Carbon Fiber. *Carbon letters* **2011**, *12*, 26-30, doi:10.5714/cl.2011.12.1.026.
26. Qin, X.; Lu, Y.; Xiao, H.; Hao, Y.; Pan, D. Improving preferred orientation and mechanical properties of PAN-based carbon fibers by pretreating precursor fibers in nitrogen. *Carbon* **2011**, *49*, 4598-4600, doi:10.1016/j.carbon.2011.06.011.
27. Wu, G.; Lu, C.; Ling, L.; Hao, A.; He, F. Influence of tension on the oxidative stabilization process of polyacrylonitrile fibers. *Journal of Applied Polymer Science* **2005**, *96*, 1029-1034, doi:10.1002/app.21388.
28. Arbab, S.; Zeinolebadi, A. A procedure for precise determination of thermal stabilization reactions in carbon fiber precursors. *Polymer Degradation and Stability* **2013**, *98*, 2537-2545, doi:10.1016/j.polymdegradstab.2013.09.014.
29. Fitzer, E.; Müller, D.J. Zur Bildung von gewinkelten Leiterpolymeren in Polyacrylnitril-Fasern. *Die Makromolekulare Chemie* **1971**, *144*, 117-133, doi:10.1002/macp.1971.021440110.
30. Simitzis, J.; Soulis, S. Correlation of chemical shrinkage of polyacrylonitrile fibres with kinetics of cyclization. *Polymer International* **2008**, *57*, 99-105, doi:10.1002/pi.2322.
31. Jing, M.; Wang, C.-G.; Zhu, B.; Wang, Y.-X.; Gao, X.-P.; Chen, W.-N. Effects of preoxidation and carbonization technologies on tensile strength of PAN-based carbon fiber. *Journal of Applied Polymer Science* **2008**, *108*, 1259-1264, doi:10.1002/app.27669.
32. Xiao, S.; Lv, H.; Tong, Y.; Xu, L.; Chen, B. Thermal behavior and kinetics during the stabilization of polyacrylonitrile precursor in inert gas. *Journal of Applied Polymer Science* **2011**, *122*, 480-488, doi:10.1002/app.33656.
33. Nunna, S.; Creighton, C.; Hameed, N.; Naebe, M.; Henderson, L.C.; Setty, M.; Fox, B.L. Radial structure and property relationship in the thermal stabilization of PAN precursor fibres. *Polymer Testing* **2017**, *59*, 203-211, doi:10.1016/j.polymertesting.2017.02.006.
34. Liu, H.C.; Chien, A.-T.; Newcomb, B.A.; Bakhtiary Davijani, A.A.; Kumar, S. Stabilization kinetics of gel spun polyacrylonitrile/lignin blend fiber. *Carbon* **2016**, *101*, 382-389, doi:10.1016/j.carbon.2016.01.096.
35. Golkarnarenji, G.; Naebe, M.; Church, J.S.; Badii, K.; Bab-Hadiashar, A.; Atkiss, S.; Khayyam, H. Development of a predictive model for study of skin-core phenomenon in stabilization process of PAN precursor. *Journal of Industrial and Engineering Chemistry* **2017**, *49*, 46-60, doi:10.1016/j.jiec.2016.12.027.
36. Nunna, S.; Naebe, M.; Hameed, N.; Fox, B.L.; Creighton, C. Evolution of radial heterogeneity in polyacrylonitrile fibres during thermal stabilization: An overview. *Polymer Degradation and Stability* **2017**, *136*, 20-30, doi:10.1016/j.polymdegradstab.2016.12.007.
37. Chai, X.; Mi, H.; Zhu, C.; He, C.; Xu, J.; Zhou, X.; Liu, J. Low-temperature thermal stabilization of polyacrylontrile-based precursor fibers towards efficient preparation of carbon fibers with improved mechanical properties. *Polymer* **2015**, *76*, 131-139, doi:10.1016/j.polymer.2015.08.049.

38. Xue, Y.; Liu, J.; Lian, F.; Liang, J. Effect of the oxygen-induced modification of polyacrylonitrile fibers during thermal-oxidative stabilization on the radial microcrystalline structure of the resulting carbon fibers. *Polymer Degradation and Stability* **2013**, *98*, 2259-2267, doi:10.1016/j.polymdegradstab.2013.08.016.

39. Bajaj, P.; Roopanwal, A.K. Thermal Stabilization of Acrylic Precursors for the Production of Carbon Fibers: An Overview. *Journal of Macromolecular Science, Part C: Polymer Reviews* **1997**, *37*, 97-147, doi:10.1080/15321799708014734.

40. Banaie, K.A.; Mirjalili, M.; Eslami-Farsani, R. The study of the correlation between ascending and descending rates of the imposed specific stress and transposition of chemical reactions during PAN precursor fibers stabilization. *Polymer Degradation and Stability* **2018**, *156*, 234-244, doi:10.1016/j.polymdegradstab.2018.09.006.

41. Sabet, E.N.; Nourpanah, P.; Arbab, S. A Novel Method for Investigation of Entropic Stress in Prestabilization of PAN-Based Precursor Fibers. *Advances in Polymer Technology* **2017**, *36*, 424-432, doi:10.1002/adv.21624.

42. Suresh, K.I.; Thomas, K.S.; Rao, B.S.; Nair, C.P.R. Viscoelastic properties of polyacrylonitrile terpolymers during thermo-oxidative stabilization (cyclization). *Polymers for Advanced Technologies* **2008**, *19*, 831-837, doi:10.1002/pat.1042.

43. Jain, M.K.; Abhiraman, A.S. Conversion of acrylonitrile-based precursor fibres to carbon fibres. *Journal of Materials Science* **1987**, *22*, 278-300, doi:10.1007/bf01160584.

44. Bashir, Z. The Hexagonal Mesophase in Atactic Polyacrylonitrile: A New Interpretation of the Phase Transitions in the Polymer. *Journal of Macromolecular Science, Part B* **2007**, *40*, 41-67, doi:10.1081/mb-100000053.

45. Yao, Z.; Wu, D.; Chen, C.; Zhang, M. Creep behavior of polyurethane nanocomposites with carbon nanotubes. *Composites Part A: Applied Science and Manufacturing* **2013**, *50*, 65-72, doi:10.1016/j.compositesa.2013.03.015.

46. McCrum, N.; Buckley, C.; Bucknall, C. *Principles of Polymer Engineering*, 2nd ed.; Cambridge University Press: Cambridge, United Kindom:, 2002.

47. Arbab, S.; Zeinolebadi, A. Quantitative analysis of the effects of comonomers and heating conditions on the stabilization reactions of polyacrylonitrile fibers as carbon fiber precursors. *Polymer Degradation and Stability* **2017**, *139*, 107-116, doi:10.1016/j.polymdegradstab.2017.04.003.

48. Bashir, Z.; Rastogi, S. The Explanation of the Increase in Slope at the Tg in the Plot of d-Spacing Versus Temperature in Polyacrylonitrile. *Journal of Macromolecular Science, Part B* **2005**, *44*, 55-78, doi:10.1081/mb-200044588.

49. Arbab, S.; Teimoury, A.; Mirbaha, H.; Adolphe, D.C.; Noroozi, B.; Nourpanah, P. Optimum stabilization processing parameters for polyacrylonitrile-based carbon nanofibers and their difference with carbon (micro) fibers. *Polymer Degradation and Stability* **2017**, *142*, 198-208, doi:10.1016/j.polymdegradstab.2017.06.026.

50. Hou, Y.; Sun, T.; Wang, H.; Wu, D. A new method for the kinetic study of cyclization reaction during stabilization of polyacrylonitrile fibers. *Journal of Materials Science* **2008**, *43*, 4910-4914, doi:10.1007/s10853-008-2713-z.

51. Farsani, E.R.; Raissi, S.; Shokuhfar, A.; Sedghi, A. FTIR Study of Stabilized PAN Fibers for Fabrication of Carbon Fibers. *World Academy of Science, Engineering and Technology* **2009**, *50*.

52. Hameed, N.; Sharp, J.; Nunna, S.; Creighton, C.; Magniez, K.; Jyotishkumar, P.; Salim, N.V.; Fox, B. Structural transformation of polyacrylonitrile fibers during stabilization and low temperature

carbonization. *Polymer Degradation and Stability* **2016**, *128*, 39-45, doi:10.1016/j.polymdegradstab.2016.02.029.

53. Liu, X.; Zhu, C.; Guo, J.; Liu, Q.; Dong, H.; Gu, Y.; Liu, R.; Zhao, N.; Zhang, Z.; Xu, J. Nanoscale dynamic mechanical imaging of the skin–core difference: From PAN precursors to carbon fibers. *Materials Letters* **2014**, *128*, 417-420, doi:10.1016/j.matlet.2014.04.176.
54. Newcomb, B.A. Processing, structure, and properties of carbon fibers. *Composites Part A: Applied Science and Manufacturing* **2016**, *91*, 262-282, doi:10.1016/j.compositesa.2016.10.018.
55. Zhao, R.-X.; Sun, P.-f.; Liu, R.-j.; Ding, Z.-h.; Li, X.-s.; Liu, X.-y.; Zhao, X.-d.; Gao, Z.-m. Influence of heating procedures on the surface structure of stabilized polyacrylonitrile fibers. *Applied Surface Science* **2018**, *433*, 321-328, doi:10.1016/j.apsusc.2017.09.252.
56. Jin, S.; Guo, C.; Lu, Y.; Zhang, R.; Wang, Z.; Jin, M. Comparison of microwave and conventional heating methods in carbonization of polyacrylonitrile-based stabilized fibers at different temperature measured by an in-situ process temperature control ring. *Polymer Degradation and Stability* **2017**, *140*, 32-41, doi:10.1016/j.polymdegradstab.2017.04.002.
57. Musiol, P.; Szatkowski, P.; Gubernat, M.; Weselucha-Birczynska, A.; Blazewicz, S. Comparative study of the structure and microstructure of PAN-based nano- and micro-carbon fibers. *Ceramics International* **2016**, *42*, 11603-11610, doi:10.1016/j.ceramint.2016.04.055.
58. Park, O.-K.; Lee, S.; Joh, H.-I.; Kim, J.K.; Kang, P.-H.; Lee, J.H.; Ku, B.-C. Effect of functional groups of carbon nanotubes on the cyclization mechanism of polyacrylonitrile (PAN). *Polymer* **2012**, *53*, 2168-2174, doi:10.1016/j.polymer.2012.03.031.
59. Fitzer, E.; Frohs, W.; Heine, M. Optimization of stabilization and carbonization treatment of PAN fibres and structural characterization of the resulting carbon fibres. *Carbon* **1986**, *24*, 387-395, doi:10.1016/0008-6223(86)90257-5.
60. Meinl, J.; Schönfeld, K.; Kirsten, M.; Kittler, K.; Michaelis, A.; Cherif, C. Optimization of the temperature program to scale up the stabilization of polyacrylonitrile fibers. *Composites Part A: Applied Science and Manufacturing* **2017**, *96*, 37-45, doi:10.1016/j.compositesa.2017.02.010.